Tribology International 154 (2021) 106720

Contents lists available at ScienceDirect

Tribology International

journal homepage: http://www.elsevier.com/locate/triboint

Friction and cutting characteristics of micro-textured diamond tools fabricated with femtosecond laser

Qingwei Wang [a,b], Ye Yang [c], Peng Yao [a,b,*], Zhiyu Zhang [d,**], Shimeng Yu [a,b], Hongtao Zhu [a,b], Chuanzhen Huang [a,b]

[a] Center for Advanced Jet Engineering Technologies (CaJET), School of Mechanical Engineering, Shandong University, Jinan, Shandong, 250061, China
[b] Key Laboratory of High Efficiency and Clean Mechanical Manufacture, Shandong University, Ministry of Education, Jinan, Shandong, 250061, China
[c] Shanghai Spaceflight Precision Machinery Institute, Shanghai, 201600, China
[d] Key Laboratory of Optical System Advanced Manufacturing Technology of the Chinese Academy of Sciences, Changchun Institute of Optics, Fine Mechanics and Physics, Chinese Academy of Sciences, Changchun, Jilin, 130033, China

ARTICLE INFO

Keywords:
Single-crystal diamond tool
Micro-texture
Wear
Femtosecond laser

ABSTRACT

Micro-textures have been preliminarily applied to reduce the wear of metallic, ceramic, and carbide tools. However, it is still unclear which micro-textures will be effective in reducing the wears of single-crystal diamond tools. In this paper, the effectivity of micro-textures on the friction and cutting characteristics of single-crystal diamond tools were verified. Four types of micro-textures including straight grooves array, concentric circular texture, ring sequence, and mesh texture were generated on the rake face of the diamond tools with the femtosecond laser. Experimental results showed that the cutting forces and friction coefficients of the micro-textured diamond tools were greatly decreased except for concentric circular texture. Meanwhile, the cutting performances of the single-crystal diamond tools were effectively improved.

1. Introduction

Due to a series of advantages, such as high strength, high hardness, high wear resistance, low friction coefficient, and chemical inertness, diamonds have been widely applied in mechanical, material, chemical, and other engineering fields [1–3]. Diamonds are also widely used as high wear-resistant devices, such as metal drawing dies, anti-wear belts for oil drill pipes, and wear-resistant valves for extreme working conditions in chemical industries [4–8]. Moreover, diamond tools sharpened with edge sharpness down to 30 nm can produce ultra-thin chips in the cutting of non-ferrous metals. Owing to its low friction coefficient, the ultra-thin chips are not prone to adhere to the diamond surface. Therefore, the diamond is a preferable tool material [9]. Although it has many excellent properties, the diamond tool is brittle and easy to be fractured during ultra-precision cutting processes [10–13].

Metal mirrors including the copper mirrors, have a wide range of applications like reflectors with a high thermal conductivity in laser applications and soft x-ray optical mirrors [14,15]. The size of the copper mirror is large (a diameter of 400 mm), and require high surface quality [16]. Single-point diamond turning is widely used for fabricating high-quality copper mirror. However, the problem of poor machining quality due to tool wear during machining has not been solved.

Tribological studies have confirmed that, micro-textured surfaces can significantly improve the friction characteristics between friction pairs [17–20]. For example, the chevron pockets with 13.02% texture density on the surface of a cemented carbide can reduce the friction coefficient by 40% [21]. The appropriate textured surfaces with oval-shaped dimples processed on the SAE1020 steel can reduce the friction coefficient by 9.4% [22]. Micro-textures also improve the friction characteristics of the cutting tools. Due to the surface texture of the tool, the speed of the lubricant will increase and contribute to forming a thicker lubricating film [23]. Meanwhile, based on lubricant film, the micro-grooves can form high-pressure lubricating film area and provide a higher thrust force to the chip. This reduces contact between the chip and the micro-bulges and decreases the cutting and friction coefficient [24]. For example, the micro-grooves on the polycrystalline diamond (PCD) tools can improve anti-adhesive ability and reduce friction coefficient by 10% combined with cryogenic minimum quantity lubrication

* Corresponding author. Center for Advanced Jet Engineering Technologies (CaJET), School of Mechanical Engineering, Shandong University, Jinan, Shandong, 250061, China.
** Corresponding author.
E-mail addresses: yaopeng@sdu.edu.cn (P. Yao), zhangzhiyu@ciomp.ac.cn (Z. Zhang).

https://doi.org/10.1016/j.triboint.2020.106720
Received 13 July 2020; Received in revised form 6 October 2020; Accepted 7 October 2020
Available online 16 October 2020

[25]. The linear grooves parallel to the main cutting edge is more effective in improving the surface quality of the carbon fiber reinforced plastics (CFRP) [26]. Moreover, lubricants play an important role in the cutting process. Using liquid and solid lubricants to fill the micro-pits array on the rake face of the carbide tools, the contact length between the tool and chip is reduced by 30% in cutting experiments [27].

Although micro-textures have been successfully applied to extend the life of carbide tools and ceramic tools, there is few relevant researches and applications of micro-textures on the single-crystal diamond tools.

It is very difficult to process micro-textures on the surface of the single-crystal diamond through conventional methods. For instance, the ion beam can process micro-textures with sub-nanoscale surface roughness, but it has a slow material removal and must be carried out in a vacuum environment [28]. The chemical reaction can change the structure and composition of the diamond surface, but the products often adhere to the diamond surface, leading to the difficulty of material removal and a loss of surface precision [29].

The femtosecond laser has a series of advantages such as high precision, high resolution, small thermal effect, relatively simple operation, and high processing efficiency. It can fabricate a wide range of materials. Meanwhile, the femtosecond laser can process diamonds in the atmospheric environment, which makes it possible to on-machine process and repair micro-textures on the diamond tools surface. Therefore, it is suitable to fabricate micro-textures on the diamond tools surface [30–32].

In this study, the femtosecond laser is applied to fabricate micro-textures on diamonds surface. Firstly, a single-crystal diamond block is textured and used in the friction and wear test to study the anti-wear effects of the micro-textures. Then, the cutting experiments of the micro-textured diamond tools are carried out to study the cutting performances.

2. Experiments

2.1. Materials

The diamond used in the experiment was the synthetic single-crystal diamond (type Ia). Meanwhile, the workpiece used in the cutting experiment was an oxygen-free copper disk with a diameter of 75 mm. The physical properties of the diamond [33] and the oxygen-free copper are listed in Table 1 and Table 2, respectively.

2.2. Machining of micro-textures

The femtosecond laser was used to process the diamond surface to obtain the micro-textures. Table 3 lists the parameters of the femtosecond laser system (Spectra-Physics Spitfire Ace ™, Newport). The femtosecond laser has an obvious threshold effect in processing of materials. Different crystal planes of single-crystal diamond have different ablation thresholds. The rake face of diamond tools used in turning test was {100}. The ablation threshold of the diamond {100} plane was 0.56 J/cm^2 measured by the hole-ablation experiment.

2.2.1. Micro-texturing the diamond block

The geometric dimensions of the diamond block are 3.5 × 3.5 × 1 mm. Based on the research of some scholars [23,34], as for the study of the groove and circular textures, we made some improvements and designed the micro-textures on the diamond block. As shown in Fig. 1, five kinds of micro-textures were processed on the single-crystal diamond block using the femtosecond laser, namely: horizontal groove sequence texture (HS) and vertical groove sequence texture (VS); concentric circular texture (CS); ring sequence texture (RS); mesh texture (MS). During processing, the laser output power was set as 0.4 mW under a scanning speed of 50 μm/s.

Table 1
Physical properties of single-crystal diamond.

Material	Hardness/ HV	Modulus/ GPa	Flexural strength/GPa	Compressive strength/GPa
Diamond	6000–10,000	900–1050	1.21–1.49	1.5–2.5

Table 2
Physical properties of oxygen-free copper.

Material	Hardness/ HV	Modulus/ GPa	Tensile strength/GPa	Shear strength/GPa
Oxygen-free copper	80–90	120	0.245–0.345	0.21

Table 3
Parameters of the femtosecond laser system.

Wavelength/nm	Pulse duration/fs	Max. output power/W	Frequency/Hz
800	35	12	1000

2.2.2. Micro-texturing the diamond tool

To determine the form, the position, and the depth of crater wear on the rake face under dry friction condition, a pre-turning experiment was carried out on the ultra-precision machining system in Section 2.4. The spindle speed and feed rates were 1000 r/min and 5 μm/r, respectively. Fig. 2(a) shows the 3D morphologies of the crater wear after a cutting distance of 11.8 km. Fig. 2(b) shows the cross-section profile corresponding to the dashed line in Fig. 2(a).

As shown in Fig. 2, the wear area on tool rake face was about 60 × 50 μm^2 away from the cutting edge with the deepest point of about 1.8 μm. The micro-textures should cover the wear area known in the pre-cutting experiment. Therefore, the micro-textures were fabricated on the rake face of the diamond tools at a distance of 10 μm away from the cutting edge, with an area of 80 × 60 μm^2 and a depth of about 100 nm. Five types of micro-textures as shown in Fig. 3 were generated: (a) linear grooves parallel to the cutting edge (PGT); (b) linear grooves vertical to the cutting edge (VGT); (c) concentric circular texture (CT); (d) ring sequence texture (RT); (e) mesh texture (MT).

2.3. Friction and wear tests on the single-crystal diamond block

As shown in Fig. 4(a), a comprehensive micro-nanomaterial mechanical characteristic test system (Nano Test Vantage$_{®}$) was used in the friction and wear test. A free-oxygen copper ball and the micro-textured single-crystal diamond block, which was consistent with the materials of the workpiece and cutting tools for turning experiments respectively, were used as the friction pair. The experimental parameters are listed in Table 4. The wear area of the copper ball-head stabilized at about 800 μm^2 after 3 h of pre-friction and wear test under the 500 mN. The maximum pressure in the tool-chip interface was 750 MPa obtained through the turning simulation. Therefore, correspond with the pressure in the turning experiment, a load of 600 mN was applied to the copper ball-head after the wear area stabilized. The frequency and friction time were 5 Hz and 600 s, respectively.

2.4. Diamond turning tests

The turning experiments were carried out on the ultra-precision machining system Moore Nanotech 350. Fig. 5 illustrates the setups. A workpiece of oxygen-free copper was fixed on the spindle. A single-crystal diamond tool with a nose radius of 0.1 mm was installed on the tool holder. The rake angle and relief angle of the single-diamond tool were 0° and 10°, respectively. The initial edge radius of the diamond tool was about 120 nm, as shown in Fig. 6.

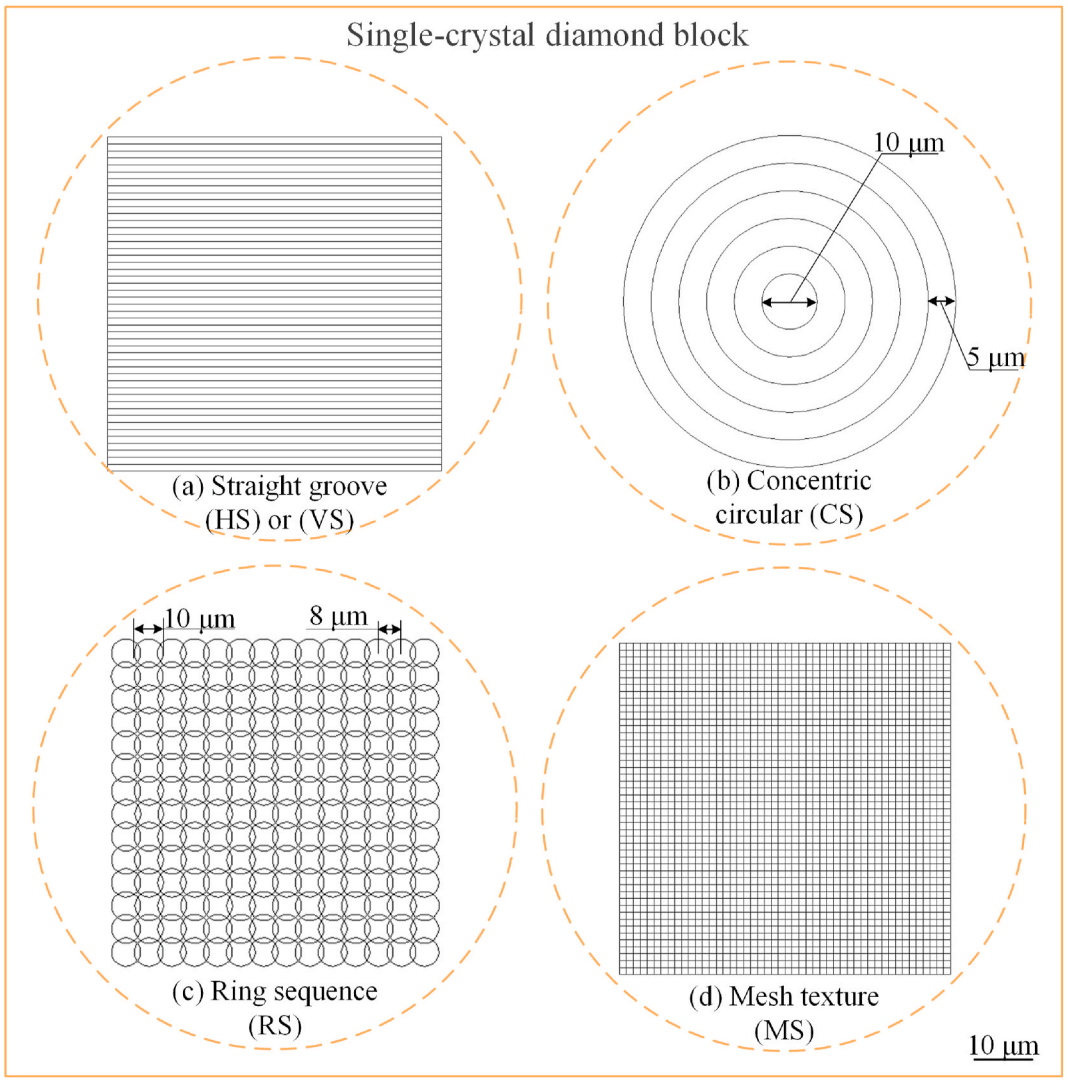

Fig. 1. Sketches of designed micro-textures on the single-crystal diamond block. The line spacing in (a) is 2.5 μm. The line-depth and line-width of the micro-textures is 100 nm and 800 nm, respectively. The position of textures on the diamond block was marked by dotted box and the shape of textures was enlarged.

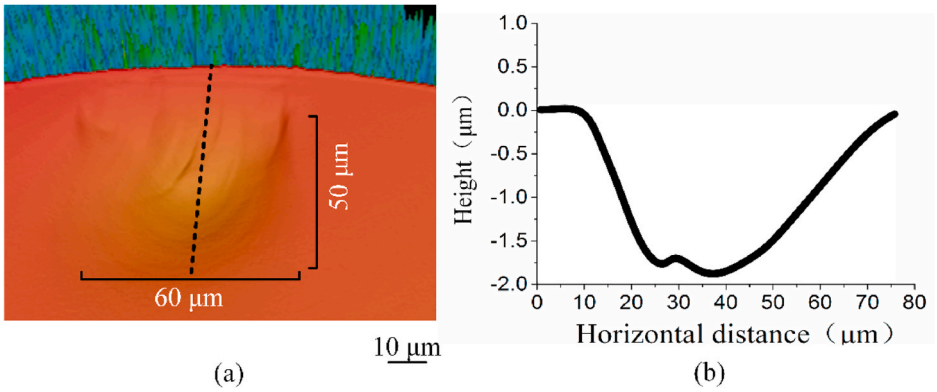

Fig. 2. Micrographs of the crater wear at rake face after the pre-cutting experiment. (a) 3D morphology, (b) 2D profile.

The turning parameters are listed in Table 5 . A dynamometer (9257B, Kistler) was fixed under the tool holder to measure the cutting forces. After turning, the surface morphologies of the tools and workpieces were examined by a 3D laser confocal microscope (VK-X200K, Keyence, Japan) and a scanning electron microscope (SEM). The profile of the cutting edge was examined by an atomic force microscope (AFM). The surface roughness of the processed workpieces was measured by the 3D laser confocal microscope.

2.5. Finite element simulation

To analyze the wear mechanism, the pressure distribution on the

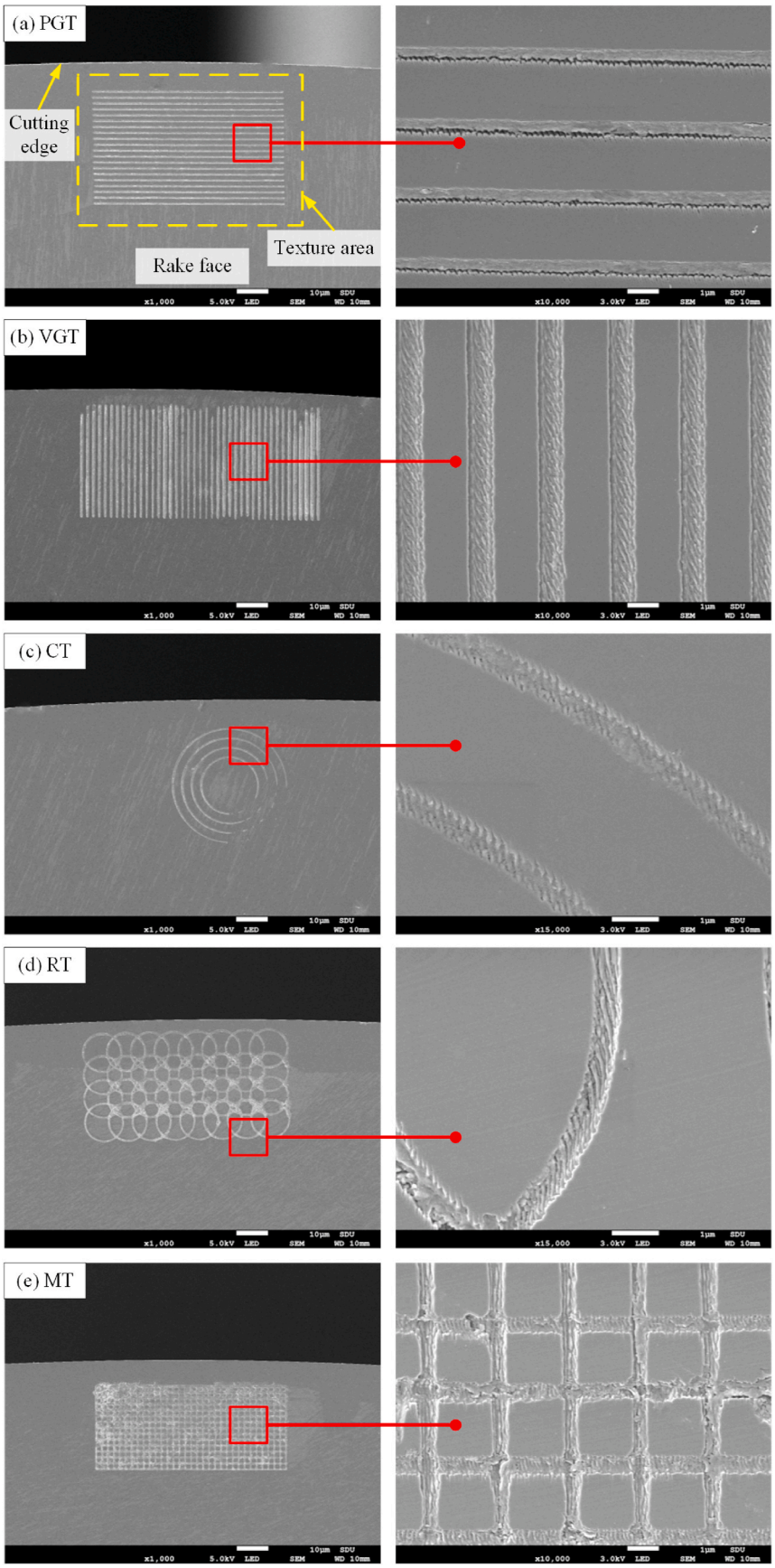

Fig. 3. SEM photographs of surface textures on tool rake face processed by femtosecond laser: (a) PGT, (b) VGT, (c) CT, (d) RT, and (e) MT.

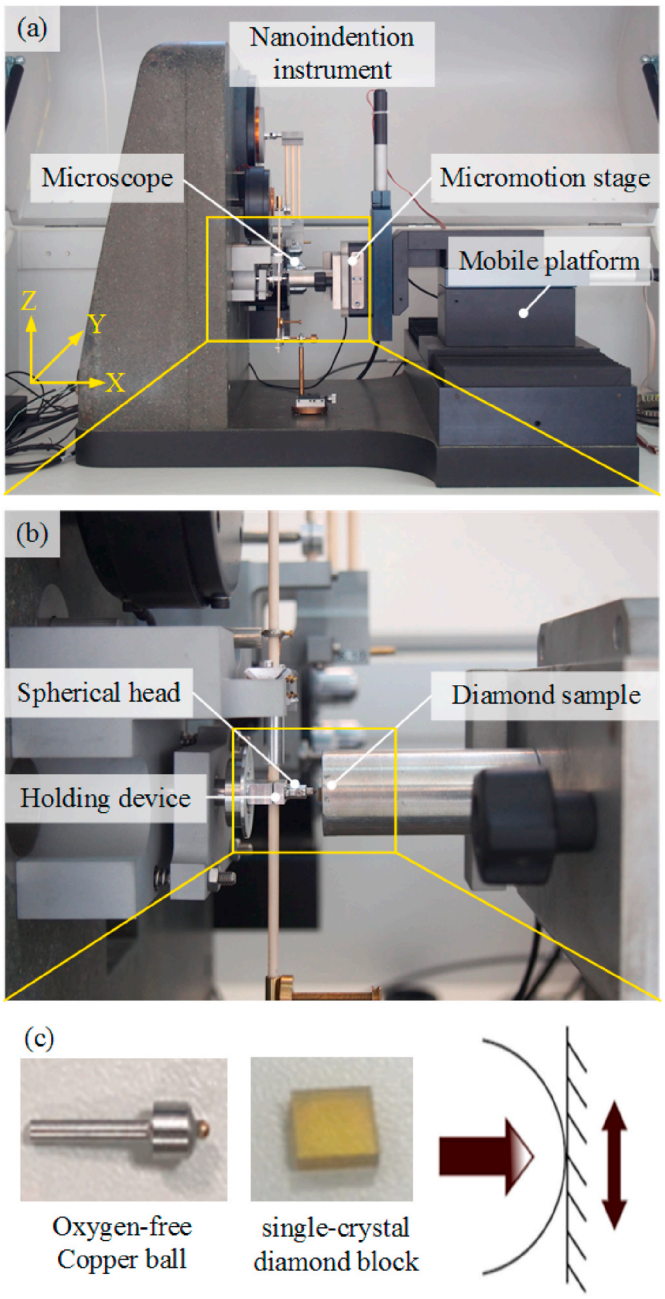

Fig. 4. (a) Comprehensive micro-nanomaterial mechanical characteristic test system. (b) local structures. (c) copper ball-head, diamond sample, and schematic diagram of friction and wear.

tools rake face was studied by finite element simulation. The 2D orthogonal cutting was used in the experiment. The parameters (cutting speed, tool rake angle, relief angle, and cutting edge radius) used in the simulation were consistent with those used in the experiment. The maximum tool element size, minimum tool element size and mesh grading are 0.5 μm, 0.05 μm and 0.4, respectively, as shown in Fig. 7.

3. Results and analysis

3.1. Friction characteristics of the micro-textured diamond block

The friction and wear tests were carried out in Fretting module. The friction forces on the surface of the micro-textured diamond blocks were obtained by the test system. Since the load on the copper ball-head is a constant, the friction coefficients of the micro-textured diamond surface are calculated from the friction forces. As shown in Fig. 8, compared with the single-crystal diamond block without micro-texture (BS), the friction coefficients of the micro-textured surface under dry friction were increased except for the surface with concentric texture. Therefore, the micro-textures cannot improve the tribological performance of the material under dry conditions. However, the friction coefficients were significantly decreased under lubrication conditions compared with dry conditions. The VS surface decreased by 40%, from 0.14 to 0.085. The VS, RS, and MS surfaces had lower friction coefficients than the BS surface, while the HS and CS surfaces had higher friction coefficients under lubrication conditions.

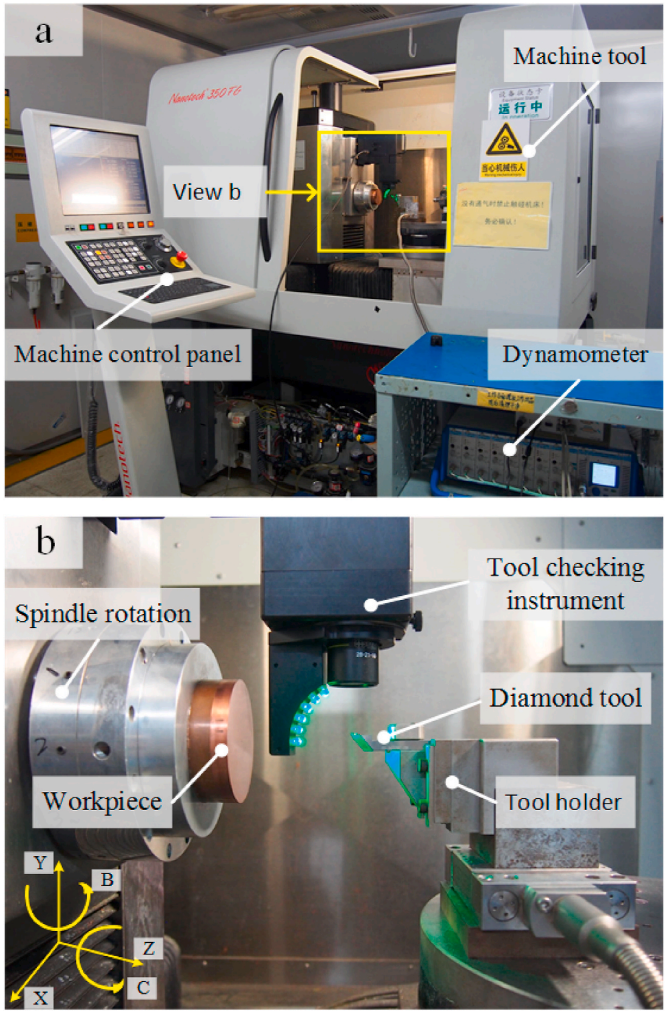

Fig. 5. Experimental setups: (a) machine tool and dynamometer. (b) tool, fixture and workpiece.

Table 4
Parameters of friction and wear experiments on the micro-textured single-crystal diamond block.

Frequency/Hz	Reciprocating stroke/μm	Load/mN	The pressure of interface/MPa	Friction time/s	Lubrication conditions	Texture types
5	15	600	750	600	Dry friction, ISOPAR-H lubricating	HS, VS, CS, RS, MS

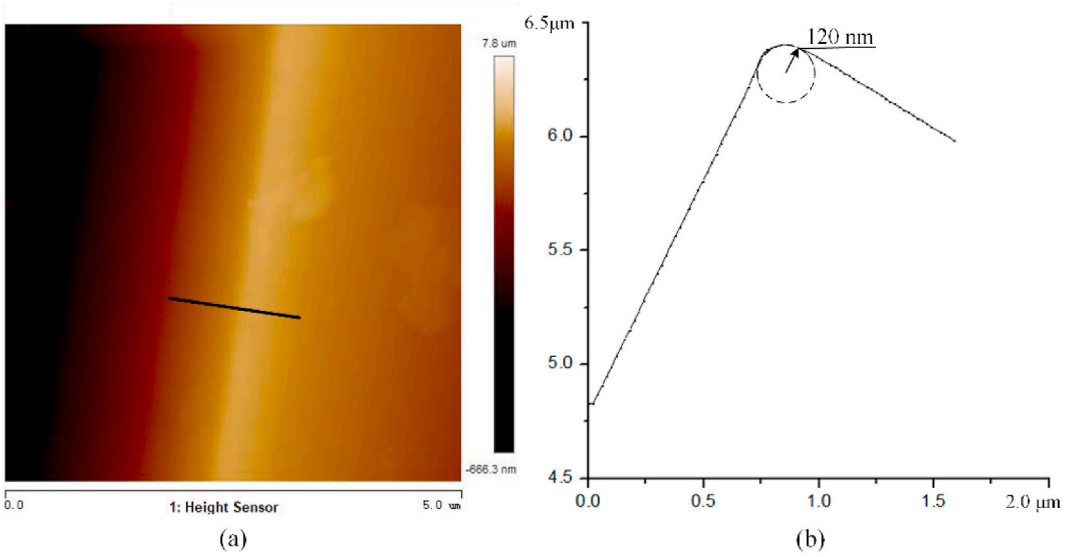

Fig. 6. The cutting edge of the diamond tools. (a) AFM photograph, (b) cross−section profile, and its fitted radius.

Table 5
Parameters of cutting tests using micro-textured single-crystal diamond tools.

Spindle speed/r/min	Feed rate/ μm/r	Depth of cut/μm	Lubrication condition	Texture types
1000	5	3	ISOPAR-H	PGT, VGT, CT, RT, MT

It is known that the wear amount increases with the number and height of contact points between friction pairs [35]. Due to the processing of micro-textures on the diamond block, the surface will appear micro-convexs and micro-grooves. Compared to the surface without micro-textures, this increases the number and height of contact points between the copper ball and diamond block. Therefore, the wear amount between the friction pairs will increase, and the tribological performance is poor under the dry conditions. Under lubrication conditions, by comparing the friction coefficients of the BS diamond surface, it is found that the friction coefficients of HS and CS surfaces slightly increased, while the friction coefficients of the other three micro-textured surfaces reduced. Because the test system is reciprocating and the groove direction of VS is parallel to the direction of the friction pair on the test system, the lubricants can spread to the diamond surface between the grooves under positive pressure. This will form a relatively stable lubricant film, which can effectively weaken the friction forces between friction pairs. On the other hand, owing to the groove direction of the HS and CS surface is not parallel to the motion direction of friction pairs, the lubricants stored in the groove are no longer under stable positive pressure, so a stable lubricating film cannot be formed. Moreover, when the copper ball passes through the groove, the contact between the copper ball and the groove edge cause the plastic deformation of the copper ball, leading to the aggravation of the adhesion effect at the contact point and an increase of friction. Considering the above two aspects, the tribological performance of HS and CS surface is poor.

3.2. Cutting characteristics of micro-textured diamond tool

3.2.1. Cutting force

Fig. 9 shows the cutting forces of the different micro-textured tools, while Fig. 10 shows the changes in cutting forces of the micro-textured diamond tools compared with the BT tool. As shown in Fig. 10, the radial thrust forces of all micro-textured diamond tools were reduced by 15%–25%. The feeding forces of PGT and CT tools were reduced by 3.8% and 5.7%, respectively. However, the feeding forces of VGT, RT, and MT tools were increased by 13.2%, 7.5%, and 18.9%, respectively. Expect for CT tool, the main cutting forces of the micro-textured diamond tools

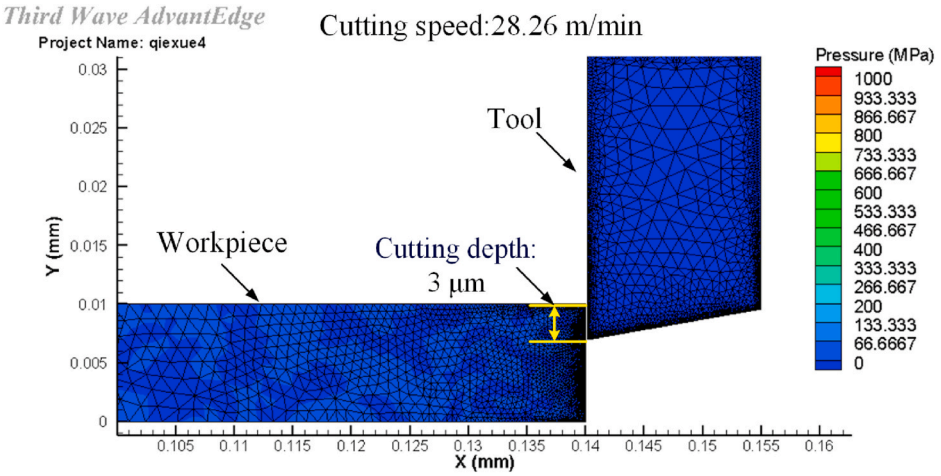

Fig. 7. The finite element simulation of 2D orthogonal cutting.

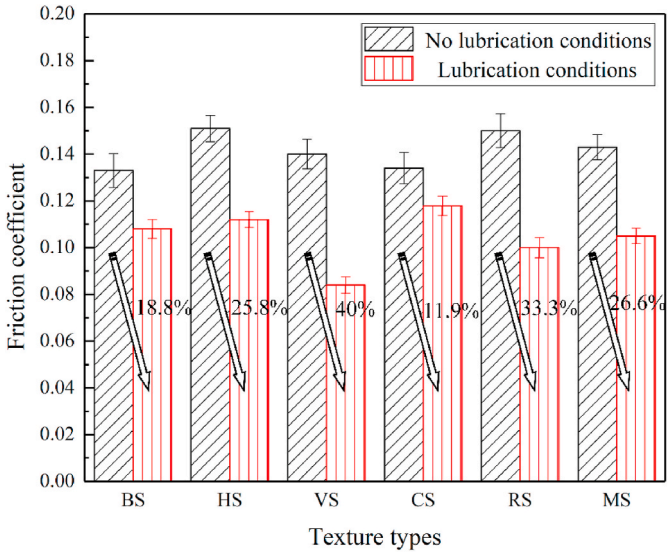

Fig. 8. Friction coefficients of different micro-textured surfaces under dry friction and lubrication conditions.

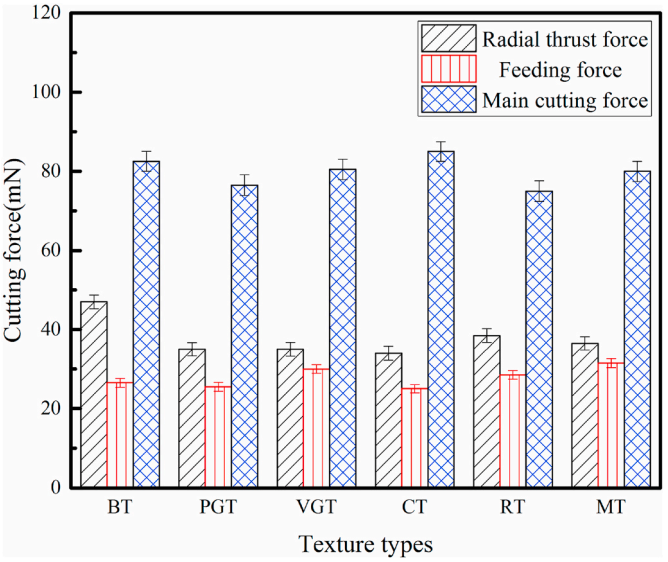

Fig. 9. Cutting forces of the different micro-textured tools.

were reduced compared with the BT tool.

3.2.2. Friction coefficient

When the friction between flank face and transitional surface or machined surface is small, the relation of the cutting force can be determined by the formula [36]:

$$F_p / F_c = \tan(\beta - \gamma_0) \quad (1)$$

The friction coefficient of the tool-chip interface can be calculated by the following equation:

$$\mu = \tan(\beta) = \tan(\gamma_0 + \arctan(F_p / F_c)) \quad (2)$$

where β is a friction angle; γ_0 is rake angle; F_p is the radial thrust force; F_c is the main cutting force.

As shown in Fig. 11, the friction coefficients of the micro-textured tools showed a decreasing trend under the lubrication condition. The friction coefficients of the PGT tool, VGT tool, and MT tool were reduced by 22.1%, 25.6%, and 20.4%, respectively. Therefore, the experimental

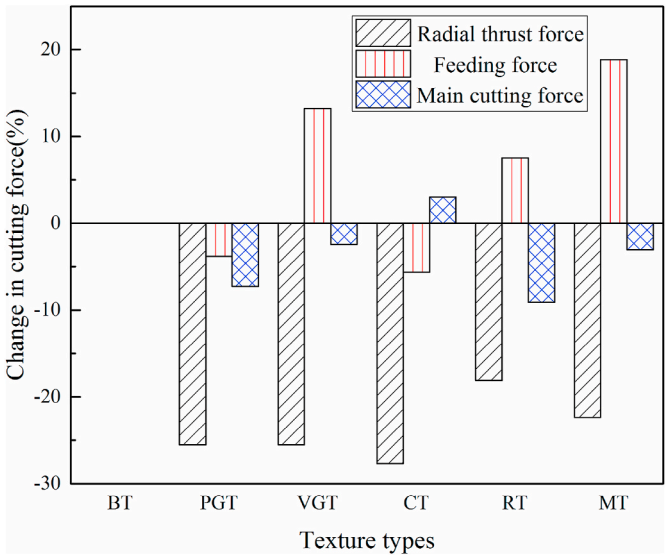

Fig. 10. Changes in cutting forces of micro-textured diamond tools compared with the BT tool.

results show that appropriate micro-textures can significantly reduce the friction coefficients of the rake face under lubrication conditions. Besides, the CT tool had the weakest reducing effect on the cutting forces and the friction coefficients of the rake face. This is probably because the concentric circular textures have a relatively large groove spacing, causing a weak ability to store lubricant and reduce the friction coefficient.

3.2.3. Surface roughness

Fig. 12 illustrates the 3D morphology of oxygen-free copper surface after the BT tool cutting. The surface roughness is measured after every four cycles of turning. As shown in Fig. 13, the surface roughness of the workpiece trended to increase with the cutting cycles. After 4 cutting cycles, the surface roughness *Ra* was around 6 nm for both micro-textured and non-micro-textured tools. After 16 cutting cycles, however, the surface roughness presented different values. As shown in Fig. 14, compared with 4 cutting cycles, the changes in surface roughness of all micro-textured tools were less than that of non-textured one after 16

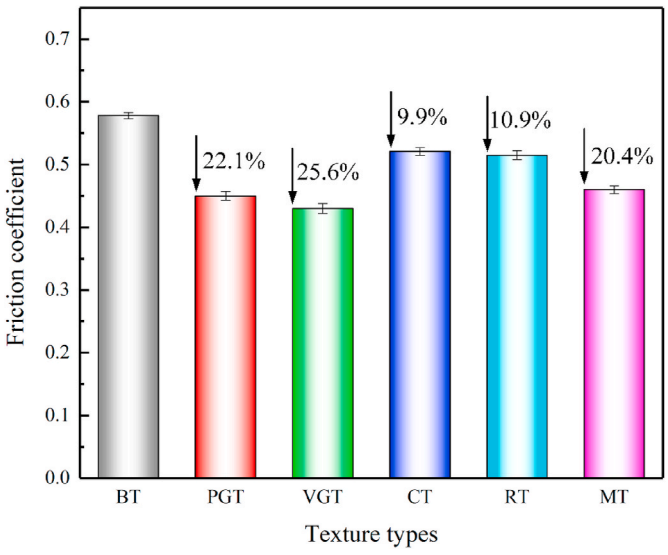

Fig. 11. Friction coefficients on the rake face of the different micro-textured diamond tools under lubrication conditions.

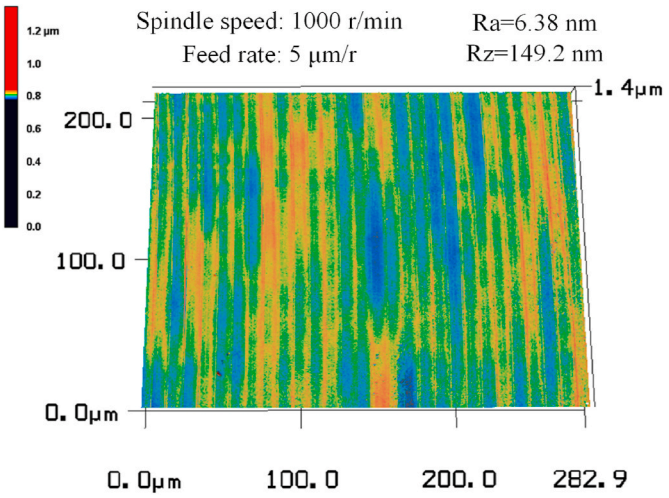

Fig. 12. Optical 3D photographs of the oxygen-free copper surface after the BT tool cutting.

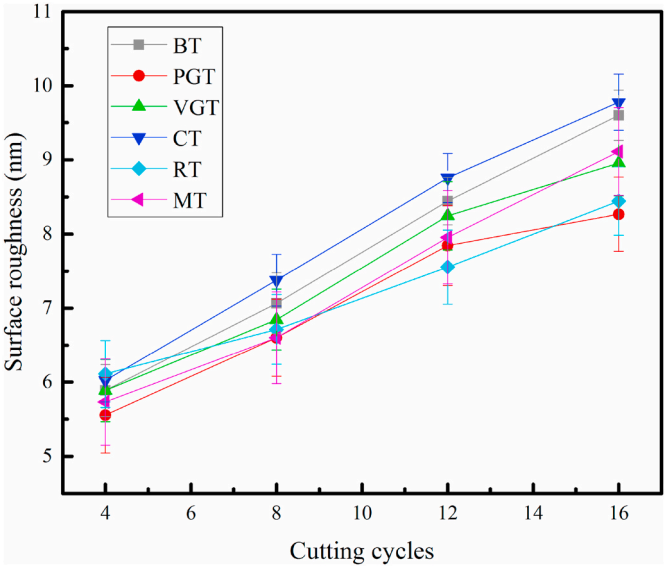

Fig. 13. The changing trend of the oxygen-free copper surface roughness with the different diamond tools.

cutting cycles. This result validates that micro-textures can effectively reduce the surface roughness of the workpiece, especially PGT, VGT, and RT textures.

3.2.4. Crater wear of rake face

Fig. 15(a) shows the wear morphology of the BT tool rake face. The crater wear was about 8 μm from the cutting edge and the maximum depth of it was around 1.2 μm. Compared with the above pre-experiment conducted with no spraying cutting fluid, the location of crater wear is roughly the same, but the wear area and the maximum wear depth slightly decrease.

Fig. 15(b–f) shows the wear morphology of the micro-textured tools rake face. For the rake face of the PGT tool, the slightest wear occurred at a distance of 70 μm from the cutting edge, with a small wear area and depth. Besides, the rake face of other micro-textured diamond cutting tools took on a similar wear condition. There was no obvious wear on the rake face, and the crater wear appeared on the right side of the textured area and away from the cutting edge.

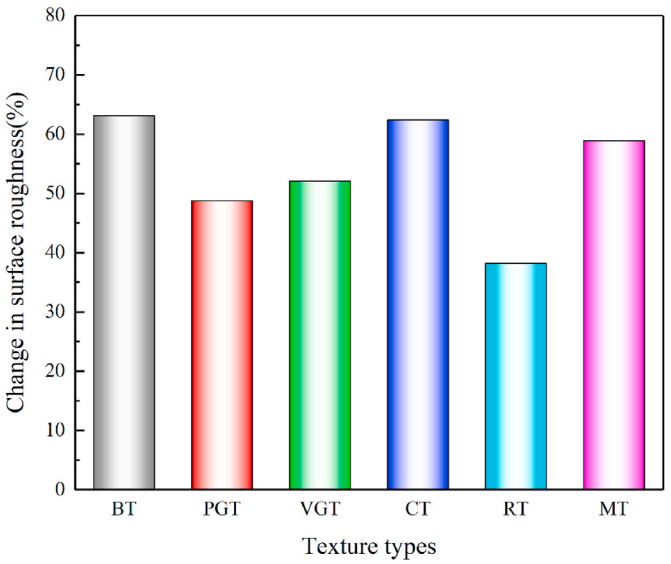

Fig. 14. The surface roughness of the oxygen-free copper cut with the different diamond tools after 16 cutting cycles.

3.2.5. Discussions

Fig. 18 shows the simulation results of the pressure distribution on the rake face. It indicates that the maximum stress is located at some distance away from the cutting edge. In fact, the crater wear of tools always starts from this location. Along with the cutting progress, the width and depth of wear land expand, and gradually reach the cutting edge. Eventually, the crater wear forms as previously shown in Fig. 2. When the crater wear is close to the cutting edge, its strength will decline sharply.

However, the crater wear will not expand to the cutting edge easily with the micro-textured diamond tools, realizing good protection to the cutting edge. Moreover, as shown in Fig. 15, the contact length of the tool and chip on the micro-textured tools increased significantly, which can reduce the pressure and average normal stress at the tool-chip interface. Research results also indicate that although the micro-textures lengthen the sliding distance of the chip, the PGT tool still shows excellent anti-wear performance.

As shown in Figs. 15-17, under lubrication conditions, the wear area, and depth of the BT tool rake face shown relatively large values. This is because there is a large pressure at the tool-chip interface, where the cutting fluid is difficult to penetrate and play its lubrication role, resulting in a poor friction reduction effect. However, there was a reduction of the wear area and depth at the tool-chip interface of the micro-textured tools, because the micro-textures improves the friction condition between the tool and chip. Due to the nature of cutting and the presence of contact points between rake face and chips, the lubricating film cannot completely separate the chip from the rake face and maintain a stable state [35]. Therefore, there are two forms of surface contact, which are the chip–rake face interaction and the chip–lubricant interaction [37]. As shown in Fig. 19, a lubrication film was formed on the tool rake face through the effect of micro-textures. A thicker and more uniform lubrication film of some micro-textured tools was formed on the tool rake face, which can effectively reduce the tool-chip friction coefficients and improve the friction performance of the tool.

Due to the existence of micro-textures, the cutting forces in the tool-chip interface have changed. Therefore, the formation and distribution of lubricating films have also changed. As for PGT, the lubricating fluid would flow away from the cutting edge under the influence of chips. However, because of the obstruction of the groove edge, some of the lubricating fluid would move towards the cutting edge, filling the plane between the grooves and forming a stable lubrication film, as shown in Fig. 19(a). As for VGT, the lubricating fluid would move away from the

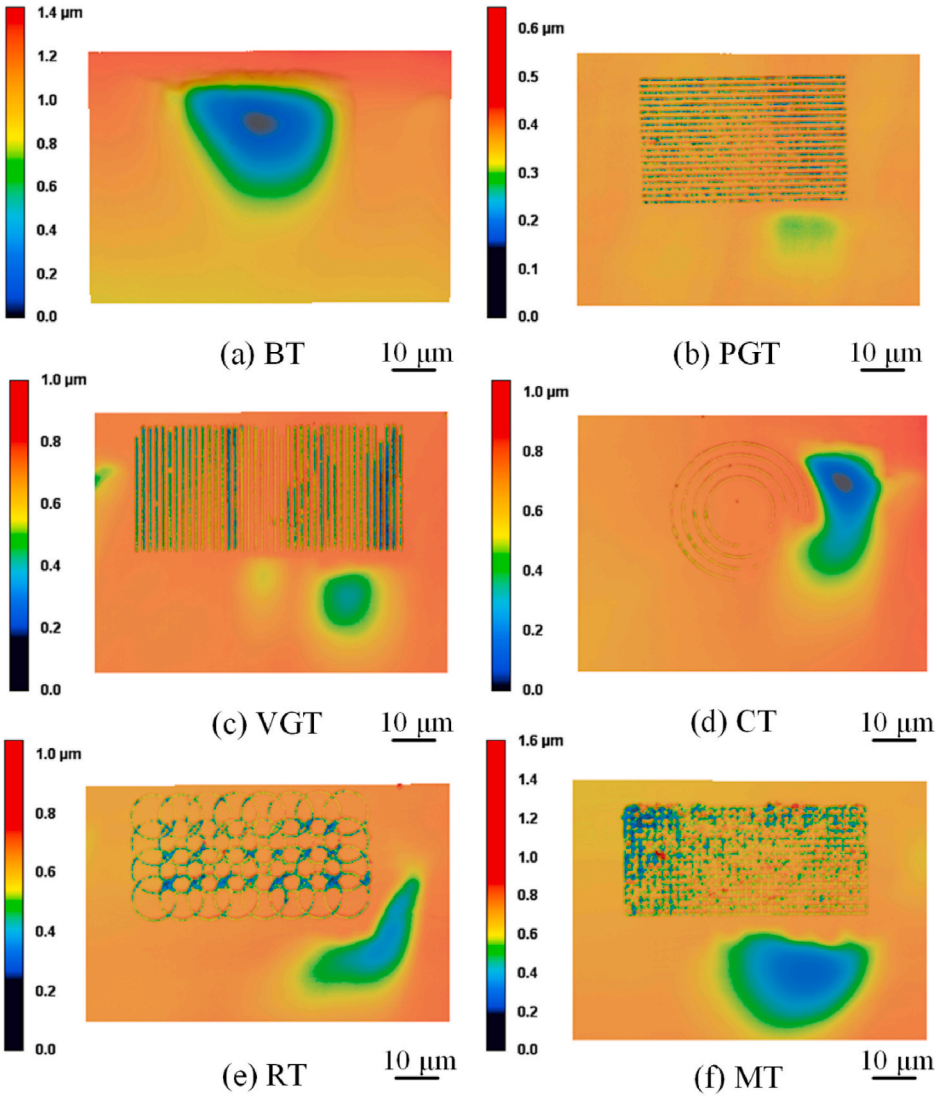

Fig. 15. Optical 3D photographs for the crater wear of the micro-textured diamond tools. For the micro-textured diamond tools, the crater wear appears on the right side of the texture area and away from the cutting edge.

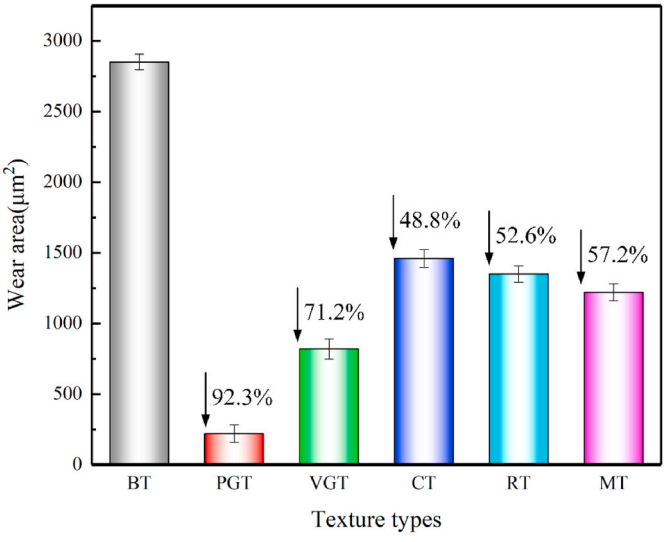

Fig. 16. The wear area on the rake face of the micro-textured diamond tools.

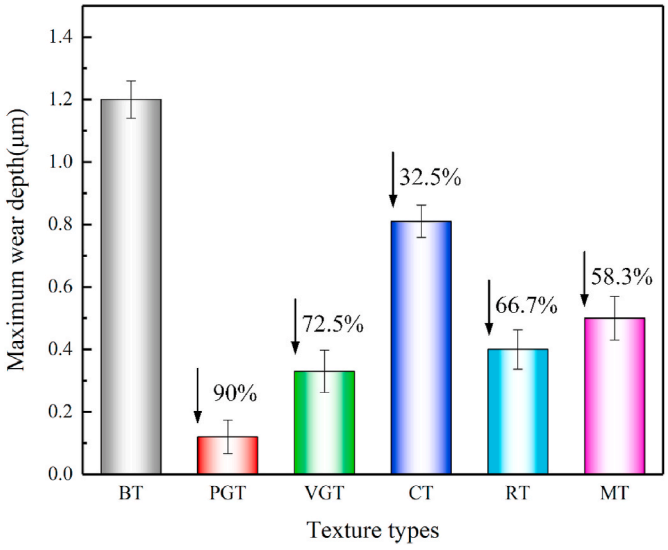

Fig. 17. The wear depth on the rake face of the micro-textured diamond tools.

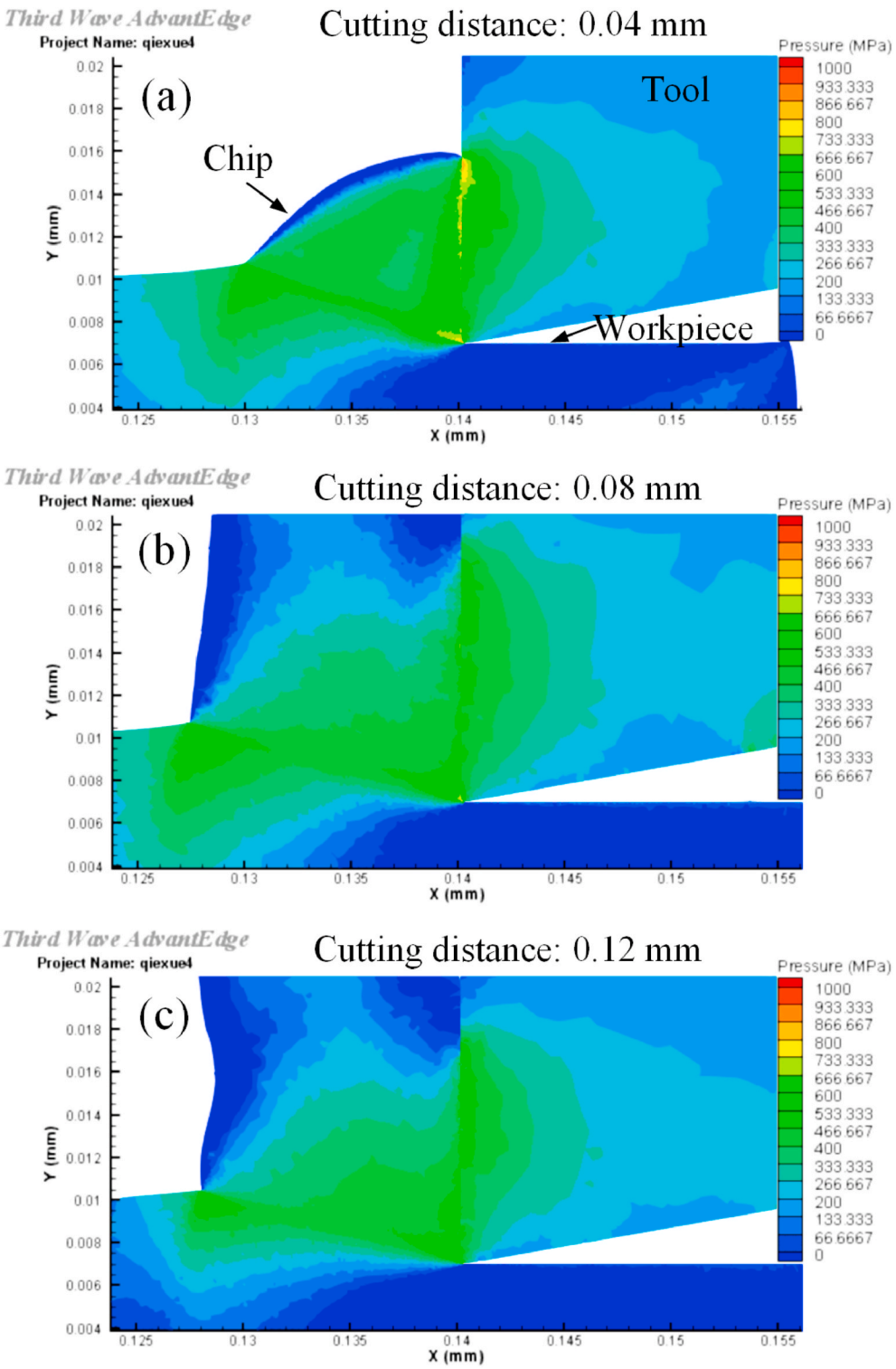

Fig. 18. Finite element simulation of the rake face pressure distribution at three different cutting distance: l = 0.04 mm (a), l = 0.08 mm (b), l = 0.12 mm (c).

cutting edge under the effect of chips. However, due to the influence of subsequent chips, the lubricating fluid in the plane would continue to move away from the cutting edge and gather on the far side of the cutting edge. Concerning CT and RT, the lubricating fluid would be blocked by the groove edge and move towards the middle of the texture, and then gather on the bottom of the ring under subsequent chip influences. The difference is that the lubricating film of the RT tool is more dispersed. Meanwhile, the MT would be divided into several block areas by grooves. Under the effect of grooves, the lubricating fluid tended to gather in the block areas and could not spread out completely.

Some scholars have studied micro-textured cutting tools to improve machining characteristics. For example, the friction reduction effect of piston surfaces mesh groove is more obvious than that of the parallel groove during the reciprocating sliding motion conditions [38]. Meanwhile, the parallel type of micro-textures improves effectively the lubrication conditions during the turning test [39]. Because the friction pair moves in different ways, our results are contrary to the results obtained by Reference 38 but are well in good agreement with Reference

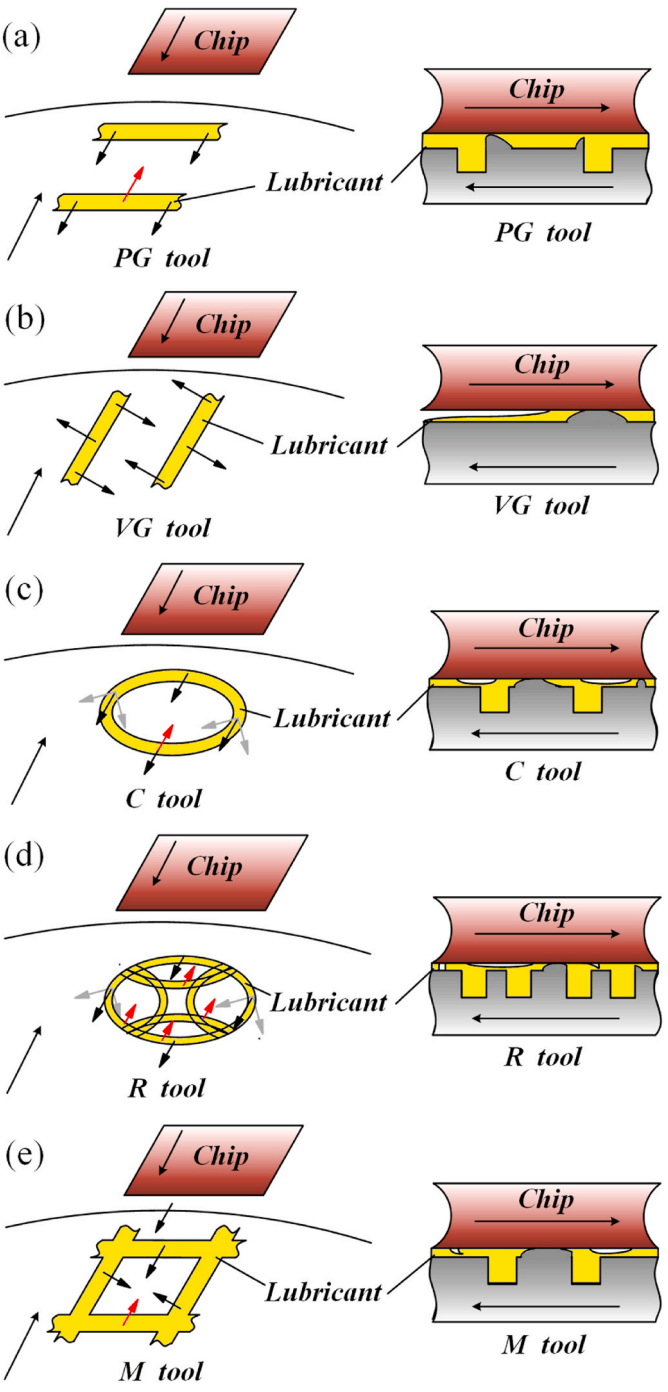

Fig. 19. Lubrication schematic diagram of five different kinds of micro-textured tools.

39. However, because friction pairs move in the same way, our results of single-crystal diamond block friction characteristics test are in agreement with Reference 38. In addition, when friction and wear tests were carried out on SAE1020 steel, high ratios of the major to the minor axis of the oval texture could result in high contact stresses which can destroy the lubricating film [22]. This has a negative effect on the life of the material. In our study, as shown in Fig. 13, CT tool has a shorter life when the surface roughness of the finished workpiece is required to be 9 nm. It is well in good agreement with Reference 22. Furthermore, the mixed texture of microscale and nanoscale can effectively improve the tool cutting performance [40]. In this paper, the size of the micro-texture was in microscale machined by femtosecond laser on the diamond tool rake face, but it also produced nanoscale texture, as shown in Fig. 3. Therefore, it will improve the diamond tool cutting performance.

The friction force F_f between the tool-chip interface can be calculated as follows [41]:

$$F_f = a_w l_f \tau_c \tag{3}$$

where a_w is the cut width; l_f is the contact length between the chip and rake face; τ_c is the average shear strength at the tool–chip interface.

When a stable lubricating film is formed, the average shear strength at the tool–chip interface will decrease compared with the dry conditions. According to the Eq. (3), the friction force will decrease. As a result, this will lead to a low friction coefficient and a small cutting force. In our study, the PGT tool rake face could form a stable oil film according to the above analysis. As for other micro-textured tools, although a stable lubricating film could not be formed on the rake face, the lubricants could be filled to the tool-chip interface. Hence, the cutting forces, average friction coefficient, and tool wear decreased more effectively. In conclusion, the friction performance of the micro-textured tools can be improved effectively.

3.2.6. *Adhesive wear of rake face*

After cutting, the micro-textured diamond tools were observed by SEM. It is known that the chip adhesion would appear on the tool rake face [42]. However, as shown in Fig. 20, there was no chip adhesion or chipping of the cutting edge. This indicated that there is no big fluctuation of cutting forces in the cutting process, which is favorable for obtaining high-quality machining surfaces. In addition, there was no significant adhesive wear at the tool-chip interface of the micro-textured tools, which indicates that micro-textures will not reduce the ability to resist adhesion of diamond cutting tools. At last, as micro-textures can gather a certain amount of chips, the abrasive wear between the chip and tool rake face might be reduced as well.

4. Conclusions

In this study, the straight groove array, concentric circular texture, ring sequence, and mesh texture were processed on the single-crystal diamond block and the diamond tool rake face by femtosecond laser. The friction and wear experiments on both the micro-textured diamond block and the diamond tool were comprehensively studied. It was found that all the micro-textures did not decrease the surface friction coefficients under dry friction, as for the micro-textured diamond block, while some did under the lubrication condition, among which the surface friction coefficient of vertical groove sequence was reduced by 40%, from 0.14 to 0.085.

In addition, under the lubrication condition, all the micro-textured diamond tools had an improved friction performance, namely the significantly reduced wear area and depth, except for that with the concentric circular texture. Meanwhile, due to the micro-textures, the crate wear was further away from the cutting edge, which could prevent the tool from early edge chipping.

Last but not least, the tool with linear grooves parallel to the cutting edge could promote a stable formation of the lubricating film in the cutting process, and hence effectively reduced the friction coefficient, surface roughness, and tool wear.

Funding

This work was supported by National Natural Science Foundation of China (Grant No. 52075302, 51775531), Shandong Provincial Natural Science Foundation (Grant No. ZR2018MEE019), and Major Basic Research of Shandong Provincial Natural Science Foundation (Grant No. ZR2018ZB0521, ZR2018ZA0401).

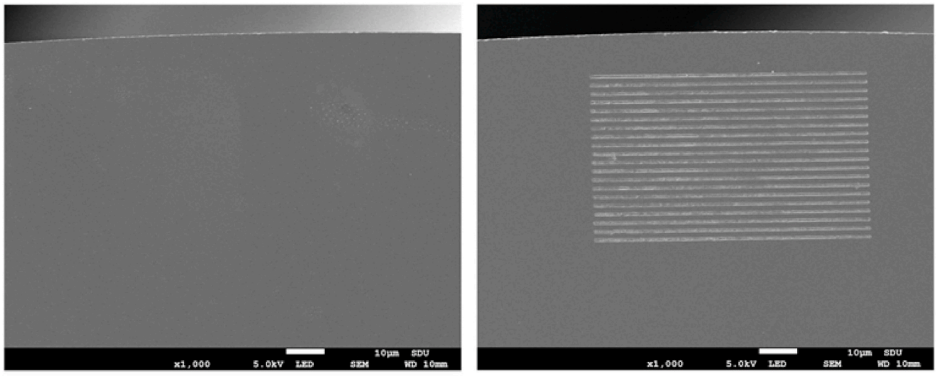

Fig. 20. SEM photograph of diamond tools rake face after cutting tests, (a) BT diamond tool rake face after cutting test, (b) VGT diamond tool rake face after cutting test.

CRediT authorship contribution statement

Qingwei Wang: Investigation, Methodology, Writing - original draft. **Ye Yang:** Writing - original draft, Data curation. **Peng Yao:** Writing - review & editing, Supervision, Project administration, Resources, Conceptualization. **Zhiyu Zhang:** Writing - review & editing, Supervision, Project administration. **Shimeng Yu:** Validation. **Hongtao Zhu:** Writing - review & editing. **Chuanzhen Huang:** Writing - review & editing.

Declaration of competing interest

The authors declare that they have no known competing financial interests or personal relationships that could have appeared to influence the work reported in this paper.

References

[1] Altukhov AA, Afanas'Ev MS, Kvaskov VB, Lyubchenko VE, Mityagin AY, Murav'Ev EN, et al. Application of diamond in high technology. Inorg Mater 2004; 40:50–70.
[2] Einaga Y. Electrochemical application of diamond electrodes. Compr Hard Mater 2014;3:493–512.
[3] Thoea TB, Aspinwallab DK, Wiseb MLH, Oxleya IA. Polycrystalline diamond edge quality and surface integrity following electrical discharge grinding. J Mater Process Technol 1996;56:773–85.
[4] Hicks ML, Pakpour-Tabrizi AC, Jackman RB. Polishing, preparation and patterning of diamond for device applications. Diam Relat Mater 2019;97. 107424.
[5] Herrmann M, Matthey B, HöHn S, Kinski I, Rafaja D, Michaelis A. Diamond-ceramics composites—new materials for a wide range of challenging applications. J Eur Ceram Soc 2012;32:1915–23.
[6] Yuan J, Lu W, Wang H, Xu F, Zuo D. Study on fabrication of diamond microstructure based on model replication technique. Rengong Jingti Xuebao 2010;39:1141–5.
[7] Gopal V, Chandran M, Rao MSR, Mischler S, Cao S, Manivasagam G. Tribocorrosion and electrochemical behaviour of nanocrystalline diamond coated Ti based alloys for orthopaedic application. Tribol Int 2016;106:88–100.
[8] Wang X, Wang C, Shen X, Sun F. Tribological properties of diamond films for high-speed drawing Al alloy wires using water-based emulsions. Tribol Int 2018;123: 92–104.
[9] Fung KY, Tang CY, Cheung CF. Molecular dynamics analysis of the effect of surface flaws of diamond tools on tool wear in nanometric cutting. Comput Mater Sci 2017; 133:60–70.
[10] Klinkova O, Rech J, Drapier S, Bergheau JM. Characterization of friction properties at the workmaterial/cutting tool interface during the machining of randomly structured carbon fibers reinforced polymer with carbide tools under dry conditions. Tribol Int 2011;44:2050–8.
[11] Zhao G, Li Z, Hu M, Li L, He N, Jamil M. Fabrication and performance of CVD diamond cutting tool in micro milling of oxygen-free copper. Diam Relat Mater 2019;100. 107589.
[12] Goel S, Luo X, Reuben RL. Wear mechanism of diamond tools against single crystal silicon in single point diamond turning process. Tribol Int 2013;57:272–81.
[13] Zhou YH. The application and performance of diamond and PCBN tools in difficult-to-cut materials. Solid State Phenom 2017;263:90–6.
[14] Zhong ZW, Lu YG. 3D characterization of super-smooth surfaces of diamond turned OFHC copper mirrors. Mater Manuf Process 2002;17:269–80.
[15] Steinkopf R, Gebhardt A, Scheiding S, Rohde A, Tünnermann M. Metal mirrors with excellent figure and roughness. SPIE-Int Soc Opt Eng Proc 2008;7102:317–47.
[16] Sollid JE, Sladky RE. Evaluation of single -point diamond -turned copper mirrors for the los alamos scientific laboratory eight -beam CO2 laser: helios. Precis Mach Opt 1978;17:586–7.
[17] Chen L, Liu Z, Shen Q. Enhancing tribological performance by anodizing micro-textured surfaces with nano-MoS_2 coatings prepared on aluminum-silicon alloys. Tribol Int 2018;122:84–95.
[18] Gajrani KK, Suresh S, Sankar MR. Environmental friendly hard machining performance of uncoated and MoS_2 coated mechanical micro-textured tungsten carbide cutting tools. Tribol Int 2018;125:141–55.
[19] Singh T, Dvivedi A. On performance evaluation of textured tools during micro-channeling with ecdm. J Manuf Process 2018;32:699–713.
[20] Menezes PL, Kishore Kailas SV. Influence of surface texture on coefficient of friction and transfer layer formation during sliding of pure magnesium pin on 080 M40 (EN8) steel plate. Wear 2006;261:578–91.
[21] Li D, Yang X, Lu C, Cheng J, Wang S, Wang Y. Tribological characteristics of a cemented carbide friction surface with chevron pattern micro-texture based on different texture density. Tribol Int 2020;142. 106016.
[22] Xu Y, Zheng Q, Abuflaha R, Olson D, Furlong O, You T, et al. Influence of dimple shape on tribofilm formation and tribological properties of textured surfaces under full and starved lubrication. Tribol Int 2019;136:267–75.
[23] Sun J, Zhou Y, Deng J, et al. Effect of hybrid texture combining micro-pits and micro-grooves on cutting performance of WC/Co-based tools[J]. Int J Adv Des Manuf Technol 2016;86:3383–94.
[24] Yin BF, Qian AQ, Lu ZT, Wang BW, Sun A. Theoretical and experimental study on lubrication performance of composite textures on cylinder liners. J Xian Jiaotong Univ 2014;48:74–80.
[25] Yang Y, Su Y, Li L, He N, Zhao W. Performance of cemented carbide tools with microgrooves in Ti-6Al-4V titanium alloy cutting. Int J Adv Manuf Technol 2015; 76:1731–8.
[26] Chen Y, Guo X, Zhang K, Guo D, Zhou C, Gai L. Study on the surface quality of CFRP machined by micro-textured milling tools. J Manuf Process 2019;37:114–23.
[27] Lei S, Devarajan S, Chang Z. A study of micropool lubricated cutting tool in machining of mild steel. J Mater Process Technol 2009;209:1612–20.
[28] Yamada I, Matsuo J, Toyoda N, Aoki T, Seki T. Progress and applications of cluster ion beam technology. Curr Opin Solid State Mater Sci 2015;19:12–8.
[29] Malshe AP, Park BS, Brown WD, Naseem HA. A review of techniques for polishing and planarizing chemically vapor-deposited (CVD) diamond films and substrates. Diam Relat Mater 1999;8:1198–213.
[30] Tsai YH, Chen BC, Ho CY, Chiou YJ, Chen KH, Chen CS, et al. Ablation characteristics of femtosecond laser processing for nanometer-sized ceramic films. Ceram Int 2017;43:3–7.
[31] Oosterbeek RN, Ward T, Ashforth S, Bodley O, Rodda AE, Simpson MC. Fast femtosecond laser ablation for efficient cutting of sintered alumina substrates. Optic Laser Eng 2016;84:105–10.
[32] Jin GX, Hu XY, Ma ZC, Li CH, Zhang YL, Sun HB. Femtosecond laser fabrication of 3D templates for mass production of artificial compound eyes. Nanotechnol Precis Eng 2019;2:110–7.
[33] Hugh OP. Handbook of carbon, graphite, diamond, and fullerenes: properties, processing, and applications. 1th ed. USA: William Andrew; 1995.
[34] Pratap T, Patra K. Mechanical micro-texturing of Ti-6Al-4V surfaces for improved wettability and bio-tribological performances. Surf Coating Technol 2018;349: 71–81.
[35] Persson BNJ, Scaraggi M. Theory of adhesion: role of surface roughness. J Chem Phys 2014;141:312–26.
[36] Lei S, Devarajan S, Chang Z. A comparative study on the machining performance of textured cutting tools with lubrication. Int J Mechatron Manuf Syst 2009;2:401–13.
[37] Ling TD, Liu P, Xiong S, Grzina D, Cao J, Wang QJ, et al. Surface texturing of drill bits for adhesion reduction and tool life enhancement. Tribol Lett 2013;52:113–22.

[38] M'Saoubi R, Chandrasekaran H. Innovative methods for the investigation of tool-chip adhesion and layer formation during machining. CIRP Ann - Manuf Technol 2005;54:59–62.
[39] Xing Y, Deng J, Zhao J, Zhang G, Zhang K. Cutting performance and wear mechanism of nanoscale and microscale textured Al2O3/TiC ceramic tools in dry cutting of hardened steel. Int J Refract Hard Met 2014;43:46–58.
[40] Obikawa T, Kamio A, Takaoka H, Osada A. Micro-texture at the coated tool face for high performance cutting. Int J Mach Tool Manufact 2011;51:966–72.
[41] Cheng RY. Principle of metal cutting. Beijing: China Machine Press; 1992.
[42] Pettersson U, Jacobson S. Textured surfaces for improved lubrication at high pressure and low sliding speed of roller/piston in hydraulic motors. Tribol Int 2007;40:355–9.